BACHELOR THESIS

SHORT-TERM EFFECTS OF ELECTRICAL STIMULI ON ENGINEERED SKELETAL MUSCLE TISSUE GROWTH

Maartje Oude Voshaar

ENGINEERING TECHNOLOGY - BIOMECHANICAL ENGINEERING

DR. J. ROUWKEMA

EXAMINATION COMMITTEE

C. Rivares Benitez, prof. Massimo Sartori and dr. J.M. Rivera Arbélaez

DOCUMENT NUMBER

 BE - 946

UNIVERSITY OF TWENTE.

17-07-2023

ABSTRACT

Muscle weakness is a common consequence of advanced disease, which can have a great impact on the patient's quality of life. The utilization of electrical stimulation in tissue engineering has shown promising outcomes in promoting skeletal muscle tissue growth and maturation. In this study, the growth characteristics of three-dimensional mouse C2C12 skeletal muscle tissue in response to electrical stimulation were researched. Electrical stimulation was performed using electrodes. The growth characteristics were assessed by evaluating the tissue structure and compaction in response to electrical stimulation.

The parameters used to measure structural changes in the skeletal muscle tissue, namely spheroid roundness and circularity, indicated no change in tissue structure over time as a result of electrical stimulation. Electrical stimulation did result in a different projection area regression model than the control group, linear and second order polynomial regression, respectively. A higher stimulation amplitude did, however, not result in a significantly different slope when comparing the 4V and 8V projection area data.

Due to spheroid adherence to the well surface and the absence of two adherence surfaces necessary for realistic mechanical stimulation, more research is needed in order to evaluate the effect of electrical stimulation on tissue growth and structural characteristics. Mechanical stimulation using two adhesion points, and evaluating tissue differentiation factors by means of qPCR analysis, is recommended for additional research.

TABLE OF CONTENTS

1 INTRODUCTION

Muscle weakness is a common consequence of advanced disease, which can have a great impact on the patient's quality of life. Neuromuscular electrical stimulation (NMES) can be beneficial when whole-body exercise is not possible. However, too little data is available on this subject to implement it on a large scale [1].

The utilization of electrical stimulation in tissue engineering has shown promising outcomes in promoting skeletal muscle tissue growth and maturation. It is known to induce various cellular responses, including increased protein synthesis, alignment of muscle fibers, and improved contractile properties [2]. However, most current research is based on in vivo and two-dimensional models. Skeletal murine myoblasts cultured as three-dimensional tissue hold great potential as in vitro models for studying realistic cell characteristics in response to stimuli [3].

In this study, the growth characteristics of mouse C2C12 skeletal muscle tissue in response to electrical stimulation were researched. The electrical stimulation was performed using electrodes. The growth characteristics were assessed by evaluating the tissue structure and compaction in response to electrical stimulation.

1.1 SKELETAL MUSCLE STRUCTURE AND FUNCTION

Muscles consist of muscle fibers bundled together in muscle fascicles. A muscle fiber is a multinucleate muscle cell consisting of myofibrils. The contractile units in myofibrils are called the sarcomeres [4]. A schematic representation of a skeletal muscle is shown in Figure 1.
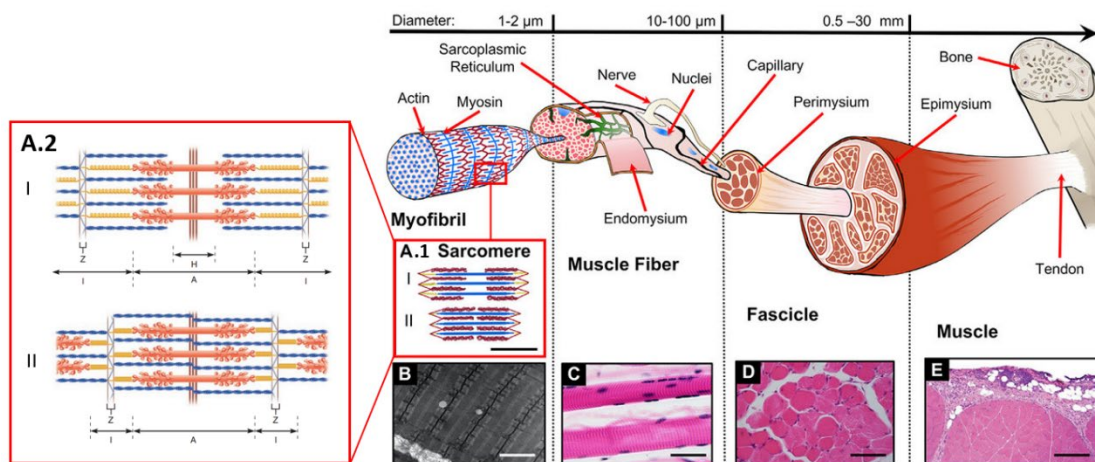
*Figure 1: Structure of skeletal muscle. **(a)** Sarcomere morphology. Actin (thin), myosin (thick) and titin (elastic) filaments are shown in (I) relaxed state and (II) during contraction. (**a.1:** [19] and **a.2:** [4]) **(b)** Transmission Electron Microscopy image of myofibrils (scalebar = 1 nm). **(c)** Phase Contrast Microscope image of two skeletal muscle fibers (scalebar = 50 μm). **(d)** Histological image of a partial fascicle cross-section (scalebar = 100 μm). **(e)** Histological image of a partial muscle cross-section (scalebar = 0.5 mm). [19]*

When stimulated by a nerve ending, the myosin and actin filaments overlap to a greater degree without changing length. Cross bridge attachments between myosin heads on thick filaments and myosin-binding sites on thin filaments form and break repeatedly, resulting in shortening of the muscle. The muscle returns to its initial length when the number of cross bridge attachments declines. One motor neuron and all the muscle fibers it innervates combined are called a motor unit.

The contraction force is described by the active tension [4]. A muscle's passive tension is generated because of mechanical stimulation. As a result, each myofibril spans the muscle fiber linearly with an

optimal sarcomere length per active contraction [5]. The elastic filament titin is the major contributor to passive tension in isolated myofibril preparations and the removal of titin diminishes virtually all passive tension [6][7].

The contractile force produced by the muscle is proportional to the myofibrillar cross-sectional area and its contractile velocity is related to the number of sarcomeres in series. Longer myofibrils contain a higher number of sarcomeres in series and their contractile velocity is therefore higher. Exercise causes an increase in myofibril number and, therefore, an increase in the contractile force of the muscle [8].

1.2 MUSCLE RESPONSE TO CHANGE IN STIMULUS FREQUENCY AND STRENGTH

A muscle twitch is the relatively fast contraction and slow relaxation as a response to a single action potential. A grated muscle response occurs when a muscle is stimulated by multiple action potentials within a short timeframe. Muscle contraction is controlled by either changing the frequency or the strength of stimulation. Contraction only occurs when stimulation strength is more than the threshold stimulus. The resulting muscle tension will increase until it reaches its maximum tension, both when increasing frequency and strength. With increasing frequency stimulation this results in a temporal summation until it reaches complete fusion. The latter is referred to as a complete tetanus [4].

1.3 RESEARCH QUESTIONS

The fundamental question that was researched is *"What are the short-term effects of low-frequency electrical stimulation on the growth characteristics of three-dimensional engineered skeletal muscle tissue (ESMT)?"*

This was divided into the following sub-questions:

1. What is the effect of electrical stimulation on engineered skeletal muscle tissue volume over time?
2. How does the skeletal muscle tissue structure change over time in response to electrical stimulation?

1.4 HYPOTHESIS

A stimulation amplitude of 8V will cause a higher muscle tension than a stimulation amplitude of 4V [4,9], which leads to the hypothesis that electrical stimulation with 8V will have a higher impact on the volume and structure of the engineered skeletal muscle tissue.

1. Exercise causes an increase in girth of the muscle, which is the result of an increase in the diameter of the muscle fibers[8]. Exercise is simulated in vitro by electrical stimulation, which therefore leads to the hypothesis that an increase in tissue volume is higher for electrically stimulated muscle tissue than for the control group.
2. Literature indicates that electrical stimulation has a positive effect on tissue growth and maturation [2]. This leads to the hypothesis that electrical stimulation will lead to an increase in tissue alignment and will therefore affect the tissue structure compared to the control group.

2 METHODOLOGY

In this chapter, the experimental plan will be presented. The initial plan is concisely described, followed by the methodology of the final plan. More details about each experimental setup can be found in the different subsections.

2.1 INITIAL EXPERIMENTAL PLAN

Figure 2 illustrates an overview of the platform upon which the experiments would have been conducted in the initial plan. Two carbon electrodes would have been positioned perpendicularly to the tissues within the well and subsequently connected to the MCS MultiChannel STG4008 stimulus generator [3].

Prior to tissue formation, C2C12 mouse myoblasts would have been cultured in cell medium and refreshed every 48*h*. On day 6, cells would have been transferred to the platform according to an adaptation of [3], wherein the cell medium would have been subsequently replaced with differentiation medium. A set of 3 tissues, one well on the platform, would have been made with a final cell quantity of 2.50×10^5 cells per tissue. Differentiation medium would have been refreshed every 24*h*.
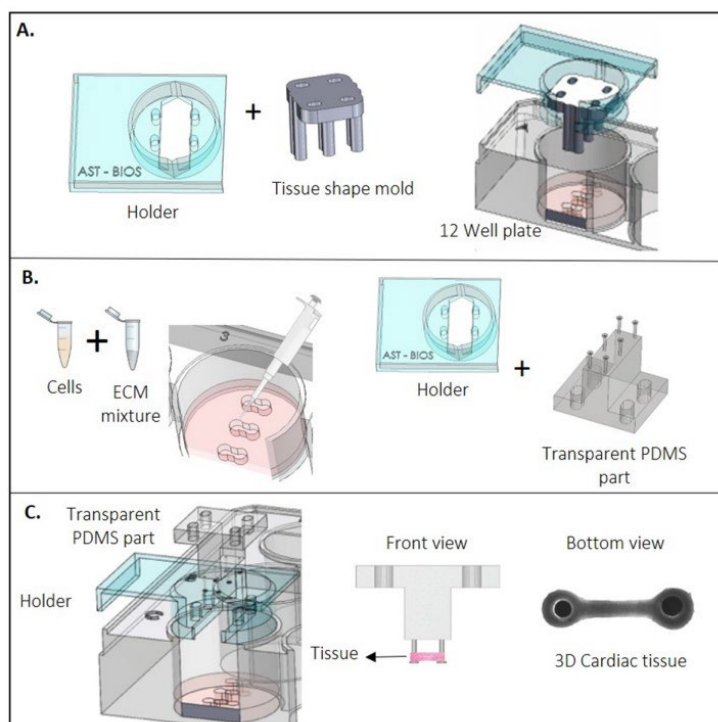
*Figure 2: ESMT formation. 36 tissues are formed on the 12 well plate, with 3 tissues per well. **(a)** Teflon tissue slots created with the use of a spacer. **(b)** Cells mixed with the supplement medium and added to the tissue slots. **(c)** Schematic overview of the platform.* [3]

2.1.1 Functional analysis

Tissue compaction, contractile force and the absence of tissue rupture would have been assessed on days 3, 7, 10, 14, 21 and 28 with a brightfield microscope to quantify the effect of electrical stimulation on functionality of the ESMT. Brightfield video analysis would have been performed by the software HAARTA, written for similar research [10].

Temporal changes in tissue volume are evaluated to assess tissue compaction. The determination of skeletal muscle tissue volume involves measuring the projection area of the tissue.

It is assumed that contraction of the tissue results in a deflection in the pillars. The HAARTA software therefore employs the elastic beam bending equation 1. to quantify the contractile force of the ESMTs [3].

$$F = \frac{3\pi E R^4}{2a^2(3L - a)}\delta \qquad (1)$$

Where F is the contraction force of the tissue (N), E is the Young's modulus of the pillars (Pa), R is the radius of a pillar (m), L is the height of a pillar (m), a is the height difference between the pillar base and the tissue attached to the pillar (m) and δ is the change in distance between the pillars caused by muscle contraction (m).

2.2 ESMT SPHEROID FORMATION

As an alternative to the utilization of the platform depicted in Figure 2, three-dimensional engineered skeletal muscle tissue was cultured in the form of spheroids (Figure 3, Figure 4). Cell culture was performed according to the Vascularization Lab protocol. C2C12 mouse myoblasts were maintained in cell medium containing high glucose DMEM (Thermo Fisher Scientific, Bremen, Germany, 41965039) supplemented with 10*%* FBS (Sigma-Aldrich, Amsterdam, Netherlands, S0615), and 1% penicillin/streptomycin (Thermo Fisher Scientific, Bremen, Germany, 15070063). Cells were cultured in a T75 culture flask (GreinerBioOne, Alphen aan den Rijn, The Netherlands, cat no. 658175) and cell medium was refreshed every 48*h* [11].

On day 4 (D4), cells were transferred to tubes (Spheroid volume experiment: GreinerBioOne, Alphen aan den Rijn, The Netherlands, cat no. 164162; Electrical stimulation experiment: GreinerBioOne, Alphen aan den Rijn, The Netherlands, cat no. 188271-N) and cell medium was substituted with differentiation medium. This differentiation medium consists of high glucose DMEM (Thermo Fisher Scientific, Bremen, Germany, 41965039) supplemented with 10% FBS (Sigma-Aldrich, Amsterdam, Netherlands, S0615) 1% penicillin/streptomycin (Thermo Fisher Scientific, Bremen, Germany, 15070063), and 2% horse serum (vendor unknown). All tubes were subjected to centrifugation at 300g for 3 minutes to facilitate the formation of spheroids, resulting in one spheroid in each tube. Differentiation medium was not refreshed between day 4 (D4) and day 7 (S3). The ESMTs were maintained at 37 °C and 5% CO_2 during the entire duration of the experiments.

2.2.1 Spheroid volume experiment

This experiment aimed to evaluate the skeletal muscle growth characteristics of spheroids in the absence of electrical stimulation (Figure 3). 36 spheroids was cultured, comprising 18 spheroids containing 1.25×10^5 cells per spheroid and an additional 18 spheroids containing 2.50×10^5 cells per spheroid. On day 7 (day 3 after spheroid formation: S3), all spheroids were transferred to two 12 well suspension culture plates (GreinerBioOne, Alphen aan den Rijn, The Netherlands, cat no. 665102); one plate containing one spheroid per well, a second plate containing two spheroids per well. A volume of $2mL$ differentiation medium was added to each well and refreshed on a daily basis between day 7 (S3) and day 14 (S10). Spheroid projection area and circularity were assessed daily using a Nikon Eclipse TS100 phase contrast microscope at a magnification of 4X, starting from day 7 (S3) and continuing until day 14 (S10).
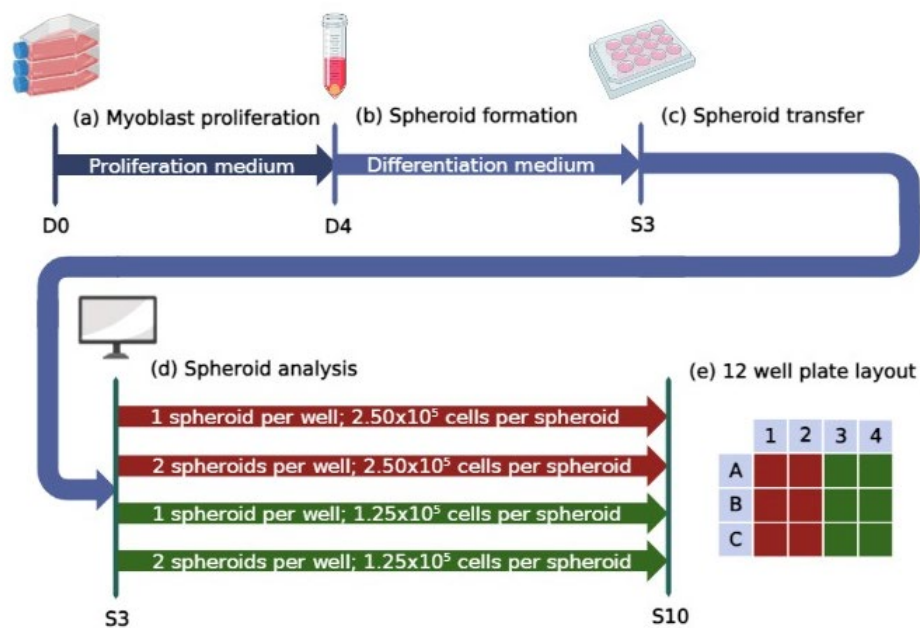
*Figure 3: Schematic representation of Experiment 1. **(a)** Myoblast proliferation in T75 culture flask until day 4 (D4). **(b)** Cell transfer to tubes and medium switch to differentiation medium until day 14 (S10). Formation of 18 spheroids containing 2.50 $x10^5$ cells per spheroid (red in (d) and (e)), and 18 spheroids containing 1.25×10^5 cells per spheroid (green in (d) and (e)). **(c)** Spheroid transfer to two 12 well plates on day 7 (S3). **(d)** Projection area, roundness and circularity assessment, every day until day 14 (S10). **(e)** Layout of both 12 well plates; one containing one spheroid per well, another containing two spheroids per well. This figure was created with BioRender [12].*

2.2.2 Electrical stimulation experiment

The second experiment was aimed to evaluate the influence of electrical stimulation on skeletal muscle characteristics. On day 4 (D4), 36 spheroids, each containing 1.25×10^5 cells, were cultured. On day 7 (day 3 after spheroid formation: S3), three spheroids per well were transferred to a 12 well suspension culture plate (GreinerBioOne, Alphen aan den Rijn, The Netherlands, cat no. 665102) containing $2mL$ differentiation medium per well. Differentiation medium was refreshed on a daily basis between day 7 (S3) and day 14 (S10).

Two carbon electrodes, spaced approximately 20mm apart, were positioned within the wells and subsequently linked to the MCS MultiChannel STG4008 stimulus generator [3]. Eight wells were electrically paced at 1Hz (4ms monophasic pulses) 16h per day, starting from day 7 (S3) and continuing until day 14 (S10). Out of these wells, four were subjected to pacing at 8V/20mm, while the remaining four were subjected to pacing at 4V/20mm. The four control wells were not subjected to electrical stimulation. This protocol is based on previous research on ESMT's response to electric pulse stimulation (EPS) [9] and is illustrated in Figure 4.

Spheroid projection area and circularity were assessed daily using a Nikon Eclipse TS100 phase contrast microscope at a magnification of 4X, starting from day 7 (S3) and continuing until day 14 (S10).
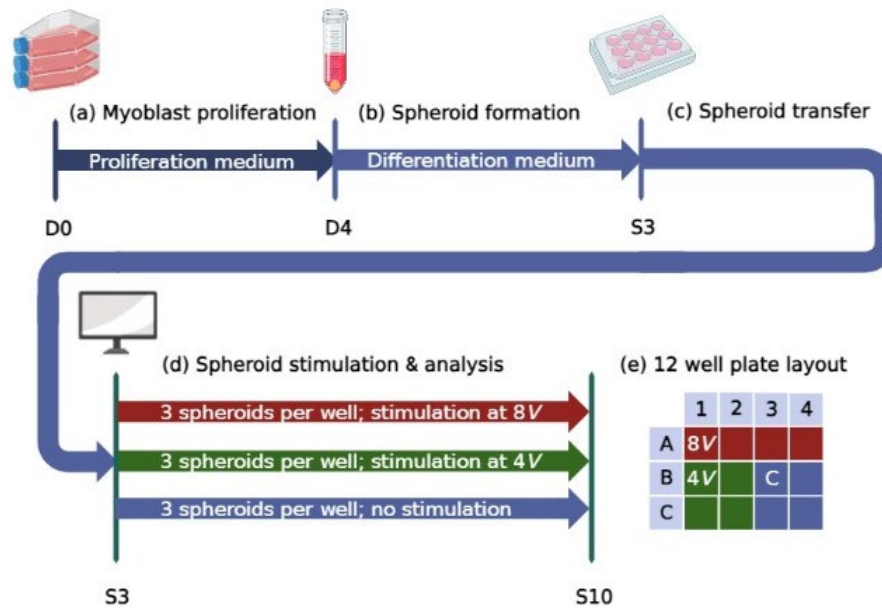
Figure 4: *Schematic representation of Experiment 2.* ***(a)*** *Myoblast proliferation in T75 culture flask until day 4 (D4).* ***(b)*** *Cell transfer to tubes and medium switch to differentiation medium until day 14 (S10). Formation of 36 spheroids containing 1.25x10^5 cells per spheroid.* ***(c)*** *Spheroid transfer to two 12 well plates on day 7 (S3).* ***(d)*** *Electrical stimulation of tissues applying 8V pulses (red), 4V pulses (green), and no stimulation (control group; blue). Projection area, roundness and circularity was assessed every day until day 14 (S10).* ***(e)*** *Layout of 12 well plate containing three spheroids per well. This figure was created with BioRender* [12]*.*

2.2.3   Functional analysis

Structure and tissue compaction is assessed with the Nikon Eclipse TS100 phase contrast microscope at 4X magnification to quantify the growth characteristics of ESMT. Functional analysis is performed by the software SpheroidJ [13]. When SpheroidJ matching was unsuccessful, the brightness via the color adjustment tool in ImageJ [14] was adjusted and subsequently particle analysis on the filtered image was performed. When color adjustment was unsuccessful due to insufficient contrast between the spheroids and the background, portions of the image were removed prior to color adjustment and particle analysis (Appendix C).

Tissue compaction was quantified by analyzing the variation in projection area of the spheroids. Spheroid roundness was monitored to evaluate the spheroid shape and formation (Equation 2):

$$R = 4\frac{A}{\pi(major\_axis)^2}$$ (2)

where R is the roundness of the spheroids, A is the actual area calculated by pixels (mm^2), and *major_axis* is the longest diameter within the spheroid (mm^2). Values approaching 1.0 indicate perfect circles. Spheroid circularity was monitored to analyze the smoothness of the spheroid surface (Equation 3):

$$C = 4\pi\frac{A}{P^2}$$ (3)

where C is the circularity of the spheroids, A is the actual area calculated by pixels (mm^2), and P is the perimeter of the spheroid (mm^2). A value of 1.0 indicates a perfect circle, while values approaching 0.0 indicate increasingly elongated polygons [15].

2.2.4   Statistical analysis

Statistical analysis is performed by GraphPad Prism 8.0.2 [16]. Statistical significant differences between data of S3 and S3 were analyzed with a 2-way ANOVA for homogeneous and Gaussian distributed data. A Kruskal-Wallis test followed by a Dunn's post hoc test was conducted on the data where these assumptions were violated.

Linear regression was performed on all data of S6-S10. When null-hypothesis (slope=0) was assumed, a Pearson correlation test was performed on homogeneous and Gaussian distributed data, while a nonparametric Spearman's rank correlation was conducted on heterogeneous and non-Gaussian distributed data to analyze the correlation between time and the parameter being tested. When the replicates test for lack of fit for linear regression indicated evidence of an inadequate model, a Goodness of Fit test was used to compare the linear regression model with a second order polynomial model.

3 RESULTS

3.1 SPHEROID VOLUME EXPERIMENT

In order to analyze the results of the volume experiment, line comparison of the projection area data per spheroid size for both 12-well plates was conducted (Appendix A). There was a significant difference in elevation of the 1.25×10^5 cells/spheroid data, $F(1, 77) = 5.057$, $p<0.05$. However, there was no significant difference between the slopes of both 12-well plates, $F(1, 76) = 3.657$, $p>0.05$. The elevation of the 2.50×10^5 cells/spheroid data was not significantly different, $F(1, 75) = 0.01446$, $p>0.05$. Similarly, the difference between the slopes of both 12-well plates was not significant either, $F(1, 76) = 3.657$, $p>0.05$.

Time and roundness were not significantly correlated for the 1.25×10^5 cells/spheroid data, $r(16) = 0.70$, $p>0.05$ and $r(58) = 0.00$, $p>0.05$ for 1 spheroid/well and 2 spheroids/well, respectively. Similarly, the correlation between time and spheroid roundness for both 12-well plates of the 2.50×10^5 cells/spheroid data was not significant, $r(16) = 0.60$, $p>0.05$ and $r(58) = 0.90$, $p>0.05$ for 1 spheroid/well and 2 spheroids/well, respectively.

The correlation between time and circularity for both 12-well plates of the 1.25×10^5 cells/spheroid data was not significant, $r(16) = 0.10$, $p>0.05$ and $r(58) = -0.70$, $p>0.05$ for 1 spheroid/well and 2 spheroids/well, respectively. Similarly, time and spheroid circularity were not correlated for the 1.25×10^5 cells/spheroid data, $r(16) = 0.20$, $p>0.05$ and $r(58) = 0.60$, $p>0.05$ for 1 spheroid/well and 2 spheroids/well, respectively.

Therefore, for both 1.25×10^5 and 2.50×10^5 cells/spheroid, the data of 1 spheroid/well are considered similar to the data of 2 spheroids per well and statistical analysis on the spheroid volume experiment data is performed on both 12-well plates combined (Figure 5).
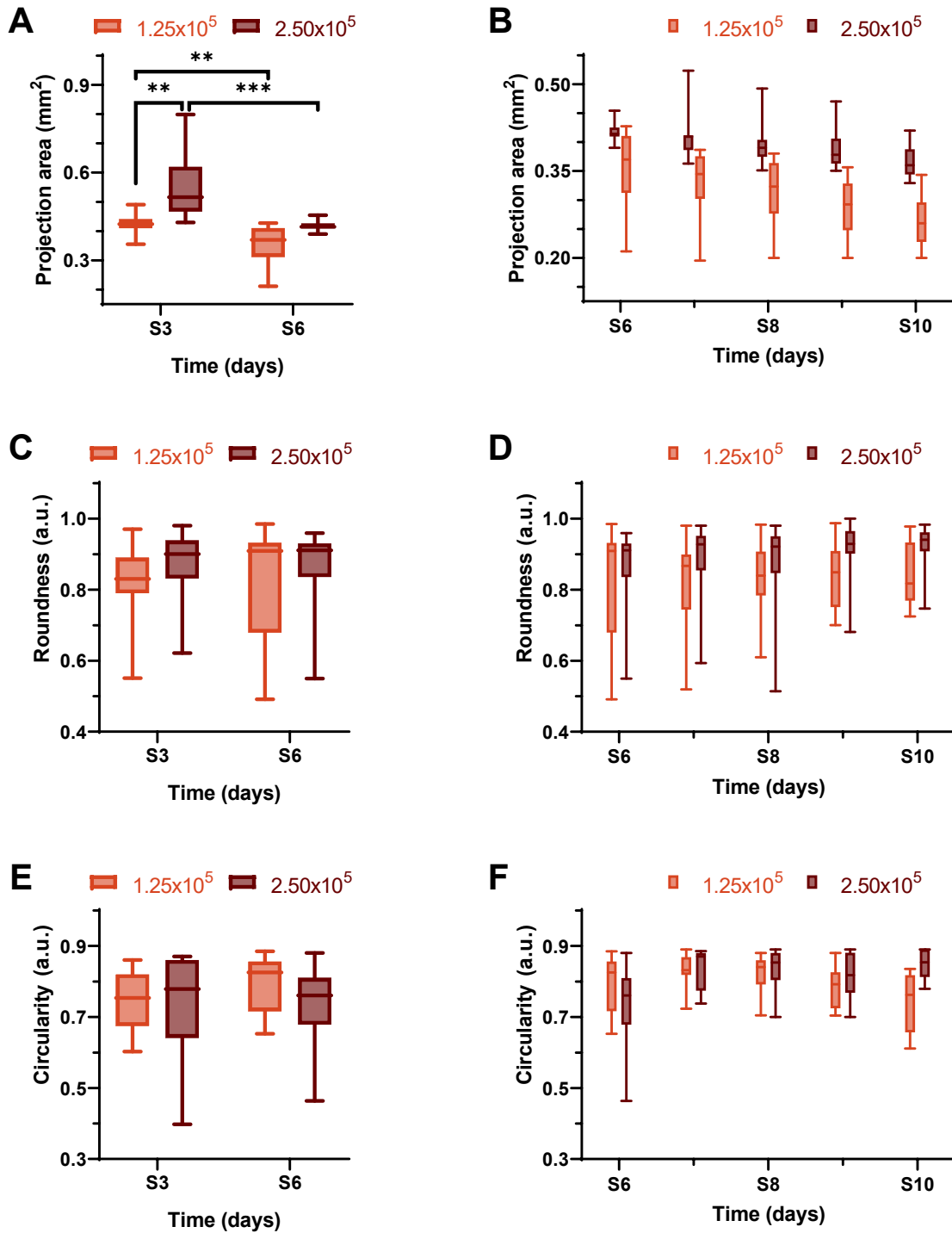
Figure 5: Spheroid volume experiment. Data are shown as means, maxima, and minima. (*A, B*) Spheroid projection area of spheroids in 1.25×10^5 and 2.50×10^5 cells/spheroid. (*C, D*) Spheroid roundness in 1.25×10^5 and 2.50×10^5 cells/spheroid. (*E, F*) Spheroid circularity in 1.25×10^5 and 2.50×10^5 cells/spheroid. In (*A, C,* and *E*), Dunn's multiple comparisons test for comparison within and between S3 and S6 was performed: * = $P < 0.05$; ** = $P < 0.01$; ***=$P < 0.001$.

It is found that on day 3 after spheroid formation (S3), the projection area of the spheroids containing 1.25×10^5 differed significantly from the projection area of the spheroids containing 2.50×10^5 cells (p=0.0034) (Figure 5A). The difference in spheroid projection area between day 3 and day 6 after spheroid formation (S3 and S6) was significant for both spheroid sizes (p=0.0060 for 1.25×10^5 cells-spheroid data; p=0.0001 for 2.50×10^5 cells/spheroid data).

However, post-hoc Dunn's multiple comparisons test indicated no significant difference in projection area between the data regarding 1.25×10^5 cells/spheroid and 2.50×10^5 cells/spheroid on S6. The Spearman correlation test indicated that time and projection area for both spheroid sizes were correlated, r(76) = -1.00, p=0.0167 for both tests. The replicates test for lack of fit regarding linear regression indicated no evidence of an inadequate model for the projection area for spheroids containing 1.25×10^5 and 2.50×10^5 cells. However, the data regarding the projection area, the roundness, and the circularity were heteroscedastic and non-Gaussian distributed. Since linear regression assumptions were violated, linear regression was considered inapplicable (Figure 5B).

Spearman correlation tests indicated that roundness and time data were not significantly correlated in both spheroid sizes, r(76) = 0.60, p>0.05 and r(76) = 0.90, p>0.05 for spheroids containing 1.25×10^5 and 2.50×10^5 cells respectively (Figure 5C, D).

Additionally, no significant correlation between time and circularity for data regarding both spheroid sizes was found, r(76) = -0.70, p>0.05 and r(76) = 0.00, p>0.05 for spheroids containing 1.25×10^5 and 2.50×10^5 cells respectively (Figure 5E, F).

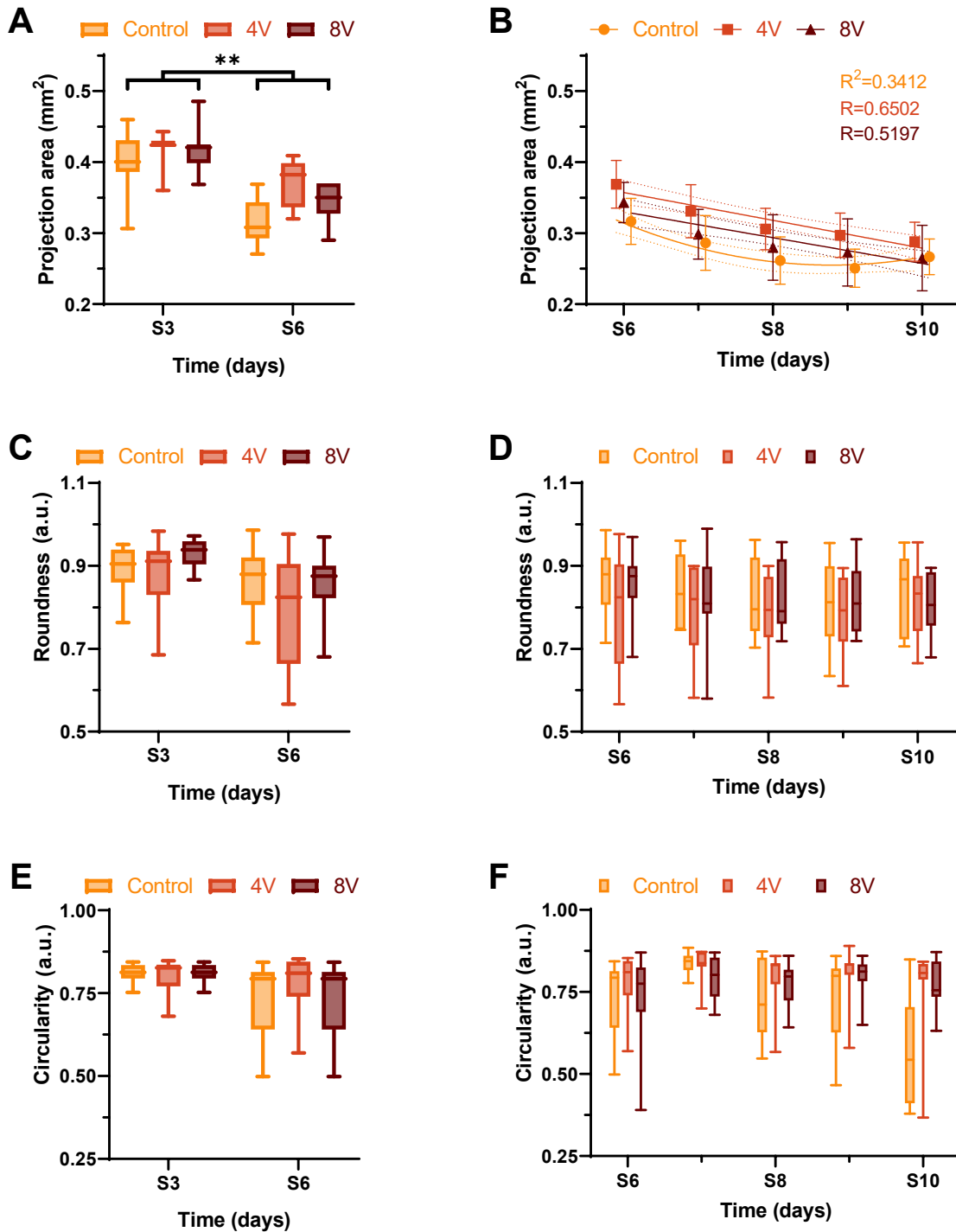## 3.2 ELECTRICAL STIMULATION EXPERIMENT

In order to compare both experiments, the projection area, the roundness, and the circularity between the spheroids containing 1.25×10^5 cells in the spheroid volume experiment (E1) and the control group in the electrical stimulation experiment (E2) were compared. The post-hoc Dunn's multiple comparisons test on both datasets showed no significant difference between both datasets regarding all three parameters. However, since linear regression assumptions were violated in E1, regression lines of both experiments could not be compared.

It is found that the difference in spheroid projection area between day 3 and day 6 after spheroid formation (S3 and S6) was significant for the spheroids in the control group and the spheroids stimulated by 8V electric monophasic pulses (p = 0.0012 for control group data; p=0.0018 for 8V stimulated spheroids data) (Figure 6A).

The replicates test for lack of fit regarding linear regression indicates no evidence of an inadequate model for the projection area for spheroids stimulated with 4V or 8V. However, this was not the case for the control group. Comparison of Fits for a second order polynomial and a straight line indicated that a straight line was the better fit for the 4V (F(1, 42) = 3.597, p=0.0648) and 8V (F(1, 57) = 3.752, p=0.0577) projection area datasets. A second order polynomial was found the better fit for the control group projection area dataset (F(1, 52) = 9.223, p=0.0037). Line comparison of 4V and 8V projection area data was conducted. There was a significant difference in elevation, F(1, 102)= 12.38, p<0.05. However, no significant difference between both slopes was found (F(1, 102) = 3.657, p>0.05) (Figure 6B).

Pearson correlation tests indicated that roundness and time data were not significantly correlated for the control (r(52) = -0.56, p>0.05) and 8V (r(57) = -0.87, p>0.05) datasets. A Spearman correlation test indicated that roundness and time data for the 4V dataset were not significantly correlated either (r(42) = 0.10, p>0.05) (Figure 6C, D).

Additionally, no significant correlation between time and circularity for control (r(52) = -0.70, p>0.05), 4V (r(42) = -0.30, p>0.05) and 8V (r(57) = 0.50, p>0.05) was found with a Spearman's rank correlation test (Figure 6E, F).

Figure 6: *Electrical stimulation experiment. (**A, B**) Spheroid projection area of spheroids containing 1.25x10^5 cells in response to no, 4V, or 8V electrical stimulation. In (**B**), data are shown as mean and standard deviation. The lines represent quadratic polynomial regression of the control data, and linear regression of the 4V and 8V data. (**C, D**) Spheroid roundness in spheroids containing 1.25x10^5 cells in response to no, 4V, or 8V electrical stimulation. (**E, F**) Spheroid circularity in spheroids containing 1.25x10^5 cells in response to no, 4V, or 8V electrical stimulation. In (**A, C, D, E,** and **F**), data are shown as means, maxima, and minima. In (**A, C,** and **E**), Dunn's multiple comparisons test for comparison within and between S3 and S6 was performed: * = P<0.05; ** = P<0.01; ***=P<0.001.*

4 DISCUSSION

In this research, the short-term effects of low-frequency electrical stimulation on the growth characteristics of three-dimensional ESMTs, spheroids, were assessed. The spheroids adhered to the well surface in both experiments, which eventually leads to two-dimensional C2C12 tissue according to literature [17]. The assumption that spheroids are spherical, which is necessary for the tissue volume calculations, was therefore violated. Nevertheless, a change in spheroid projection area is still proportional to a change in its volume.

In the first experiment (E1), the projection area, roundness, and circularity of spheroids containing 1.25×10^5 cells and 2.50×10^5 cells was followed during 7 days without electrical stimulation. In the second experiment (E2), the effect of electrical stimulation (4V and 8V monophasic pulses) on the projection area, roundness, and circularity of spheroids containing 1.25×10^5 cells was assessed. It was found that both roundness and circularity were not significantly correlated with time in both spheroid sizes in E1. Similarly, the data of both electrical stimulation amplitudes and control group in E2 showed no significant correlation between roundness and time, and circularity and time. This, however, contradicts the hypothesis that electrical stimulation would affect the tissue structure. The spheroid adherence to the well surface causes a contrast gradient between the spheroid surface and the cells proliferating on the surface of the 12-well plates (Appendix C). This phenomenon might have affected the spheroid circularity and roundness. Nevertheless, opting for alternative parameters to evaluate alterations in tissue structure could potentially yield superior outcomes. In vitro, myofibers are aligned in order to maximize contractile force. C2C12 is a myoblast cell line. Myogenesis of the cells is therefore necessary in order to maximize the contractile force of the tissue. Assessment of myogenesis can be achieved by evaluating myogenic differentiation factors, including MyoD or the myosin heavy chain. Since spheroids containing 1.25×10^5 or 2.50×10^5 cells were too large to transmit the light, live staining will only be useful when conducting experiments on smaller spheroids. The exact maximum spheroid size for live staining to be effective is therefore dependent on the microscope being used. Another method of following the expression of differentiation factors is to perform quantitative polymerase chain reaction (qPCR) on the used medium after medium refreshment, which is non-invasive and is not restricted by spheroid size [2].

Additionally, the projection area of the spheroids was followed for 7 days. The projection area of the control group in E2 followed a second order polynomial regression, while the datasets of the spheroids stimulated with 4V and 8V monophasic pulses followed a linear regression. The linear regression slopes of the data regarding spheroids stimulated with 4V and spheroids stimulated with 8V were not significantly different. This lead to the conclusion that 8V electrical stimulation did not have a significantly different effect on the spheroid growth compared to 4V stimulation. This contradicts the hypothesis that a higher stimulation amplitude will cause a greater increase in tissue volume. Due to the spheroid adhesion to the well surface, a decline in the projection area was not necessarily caused by spheroid compaction. Adherence to the well surface resulted in one adherence point for mechanical stimulation. According to literature, mechanical stimulation by means of two adherence points have a great positive influence on skeletal muscle tissue contractile and growth characteristics [6][18][8].

Therefore, additional research on mechanically stimulated three-dimensional skeletal muscle tissue is necessary in order to evaluate the effects of electrical stimulation on the growth characteristics. Since spheroids deform into two-dimensional tissue when adhering to a surface, spheroids are inadequate three-dimensional engineered tissues when performing the experiments on a non-coated 12-well plate. An alternative to spheroids would be to culture tissues between two structures, similar to the initial plan (1.1 Initial experimental plan). When evaluating the effect of electrical stimulation on the

differentiation of the tissues, expression of differentiation factors can be assessed by performing qPCR on the used medium after refreshments. This, combined with mechanical stimulation with two adherence points, is therefore recommended for additional research.

5 CONCLUSION

This research studied the short-term effects of low-frequency electrical stimulation on the growth characteristics of three-dimensional engineered skeletal muscle tissue. The parameters used to measure structural changes in the skeletal muscle tissue, namely spheroid roundness and circularity, indicated no change in tissue structure over time because of electrical stimulation. Electrical stimulation did result in a different projection area regression model than the control group, linear and second order polynomial regression, respectively. A higher stimulation amplitude did, however, not result in a significantly different slope when comparing the 4V and 8V projection area data.

Due to spheroid adherence and the absence of two adherence surfaces necessary for realistic mechanical stimulation, additional research is needed in order to further evaluate the effect of electrical stimulation on tissue growth and structural characteristics. Mechanical stimulation using two adhesion points, and evaluating tissue differentiation factors by means of qPCR is recommended for additional research.

BIBLIOGRAPHY

[1]   Jones S, Man WDC, Gao W, Higginson IJ, Wilcock A, Maddocks M. Neuromuscular electrical stimulation for muscle weakness in adults with advanced disease. Cochrane Database Syst Rev 2016;10. doi:10.1002/14651858.CD009419.PUB3.

[2]   Mueller C, Trujillo-Miranda M, Maier M, Heath DE, O'Connor AJ, Salehi S. Effects of External Stimulators on Engineered Skeletal Muscle Tissue Maturation. Adv Mater Interfaces 2021;8:2001167. doi:10.1002/ADMI.202001167.

[3]   Ribeiro MC, Rivera-Arbeláez JM, Cofiño-Fabres C, Schwach V, Slaats RH, Ten Den SA, Vermeul K, van den Berg A, Pérez-Pomares JM, Segerink LI, Guadix JA, Passier R. A New Versatile Platform for Assessment of Improved Cardiac Performance in Human-Engineered Heart Tissues. J Pers Med 2022;12. doi:10.3390/JPM12020214.

[4]   Marieb AN, Hoehn K. Human Anatomy & Physiology. 10th ed. PEARSON; 2016.

[5]   Lemke SB, Schnorrer F. Mechanical forces during muscle development. Mech Dev 2017;144:92–101. doi:10.1016/J.MOD.2016.11.003.

[6]   Bartoo ML, Linke WA, Pollack GH. Basis of passive tension and stiffness in isolated rabbit myofibrils. Am J Physiol 1997;273. doi:10.1152/AJPCELL.1997.273.1.C266.

[7]   Leonard TR, Herzog W. Regulation of muscle force in the absence of actin-myosin-based cross-bridge interaction. Am J Physiol Cell Physiol 2010;299. doi:10.1152/AJPCELL.00049.2010.

[8]   Goldspink G. Alterations in Myofibril Size and Structure During Growth, Exercise, and Changes in Environmental Temperature. Compr Physiol 1983:539–54. doi:10.1002/CPHY.CP100118.

[9]   Chen W, Nyasha MR, Koide M, Tsuchiya M, Suzuki N, Hagiwara Y, Aoki M, Kanzaki M. In vitro exercise model using contractile human and mouse hybrid myotubes. Sci Rep 2019;9. doi:10.1038/S41598-019-48316-9.

[10]   Rivera-Arbeláez JM, Keekstra D, Cofiño-Fabres C, Boonen T, Dostanic M, ten Den SA, Vermeul K, Mastrangeli M, van den Berg A, Segerink LI, Ribeiro MC, Strisciuglio N, Passier R. Automated assessment of human engineered heart tissues using deep learning and template matching for segmentation and tracking. Bioeng Transl Med 2023;8:e10513. doi:10.1002/BTM2.10513.

[11]   University of Twente. Vascularization Lab - Protocols n.d.

[12]   Scientific Image and Illustration Software | BioRender n.d. https://www.biorender.com/ (accessed June 26, 2023).

[13]   Lacalle D, Castro-Abril HA, Randelovic T, Domínguez C, Heras J, Mata E, Mata G, Méndez Y, Pascual V, Ochoa I. SpheroidJ: An Open-Source Set of Tools for Spheroid Segmentation. Comput Methods Programs Biomed 2021;200:105837. doi:10.1016/J.CMPB.2020.105837.

[14]   Schneider CA, Rasband WS, Eliceiri KW. NIH Image to ImageJ: 25 years of image analysis. Nat Methods 2012 97 2012;9:671–5. doi:10.1038/nmeth.2089.

[15]   Evaluation of Spheroid Formation and Robustness using Millicell® Ultra-low Attachment Plates n.d. https://www.sigmaaldrich.com/NL/en/technical-documents/technical-article/cell-culture-and-cell-culture-analysis/3d-cell-culture/millicell-ultra-low-attachment-plates (accessed July 9, 2023).

[16]   Rivera-Arbeláez JM, Cofiño-Fabres C, Schwach V, Boonen T, ten Den SA, Vermeul K, van den Berg A, Segerink LI, Ribeiro MC, Passier R. Contractility analysis of human engineered 3D heart tissues by an automatic tracking technique using a standalone application. PLoS One 2022;17. doi:10.1371/JOURNAL.PONE.0266834.

[17]   Jin G-Z, Ji G-Z. Enhanced growth and myogenic differentiation of spheroid-derived C2C12 cells. Biosci Biotechnol Biochem 2021;85:1227–34. doi:10.1093/BBB/ZBAB018.

[18]   Herzog W. The multiple roles of titin in muscle contraction and force production. Biophys Rev 2018;10:1187. doi:10.1007/S12551-017-0395-Y.

[19]   Gotti C, Sensini A, Zucchelli A, Carloni R, Focarete ML. Hierarchical fibrous structures for muscle-inspired soft-actuators: A review. Appl Mater Today 2020;20. doi:10.1016/J.APMT.2020.100772.

6 APPENDICES

A. VOLUME EXPERIMENT PLATE COMPARISON
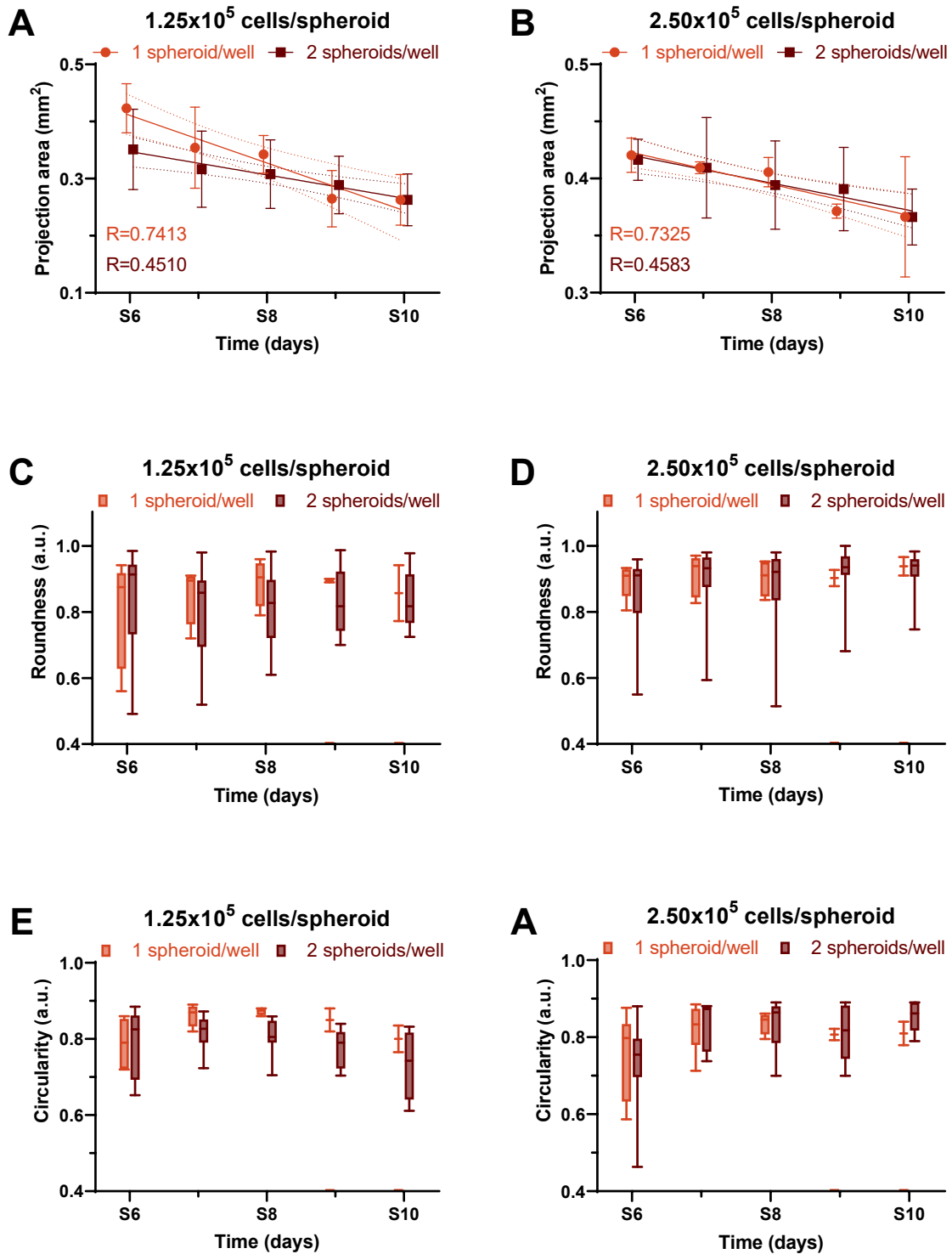
Figure 7: *Plate comparison in the spheroid volume experiment. (A, B) Spheroid projection area of spheroid in 1.25x10⁵ and 2.50x10⁵ cells/spheroid. Data are shown as mean and standard deviation with lines representing linear regression. (C, D) Spheroid roundness in 1.25x105 and 2.50x10⁵ cells/spheroid. (E, F) Spheroid circularity in 1.25x10⁵ and 2.50x10⁵ cells/spheroid. In (C, D, E, and F), data are shown as means, maxima, and minima.*

B. Comparison volume experiment and electrical stimulation control on S3
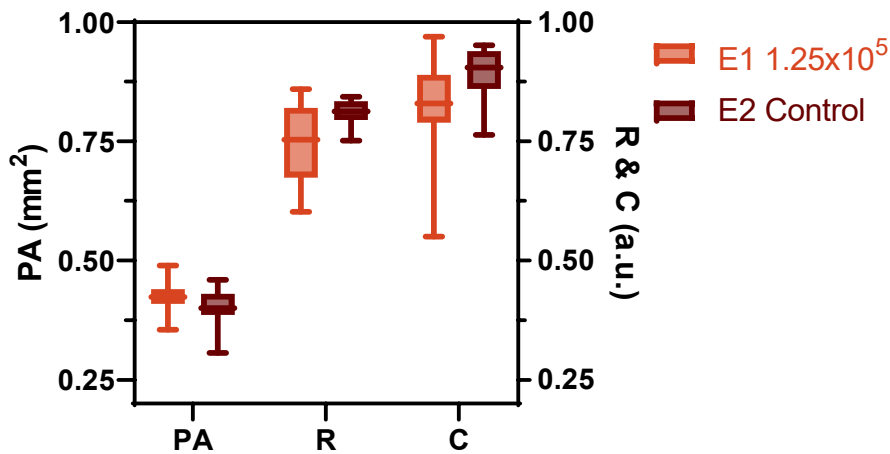
Figure 8: *Projection area (PA), roundness (R), and circularity (C) comparison between the spheroids containing 1.25x105 cells in the spheroid volume experiment (E1) and the control group in the electrical stimulation experiment (E2). Dunn's multiple comparisons test was performed on both datasets regarding the PA, R, and C: * = P<0.05; ** = P<0.01; ***=P<0.001. Data showed no significant differences.*

C. Spheroid photos

Original photos are shown on the left and the spheroid perimeter images are shown on the right. Outline images are computed with ImageJ, while the yellow line in the photos on the right indicate the spheroid outline computed by SpheroidJ. Images analyzed with ImageJ were were color adjusted by changing the brightness function in the color adjustment tool in ImageJ. However, when contrast difference was not high enough for adequate spheroid detection, sections of the image were manually deleted. Filtered images are shown as red shapes on the location of the speroid, while deletions are indicated as is shown in Figure 9. Magnification is 4X unless otherwise indicated.
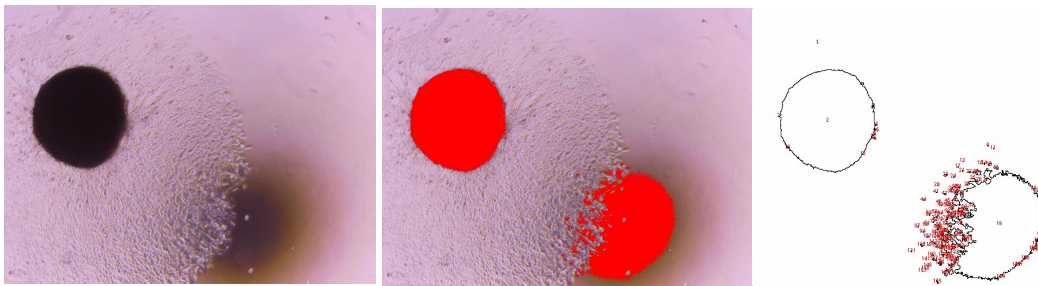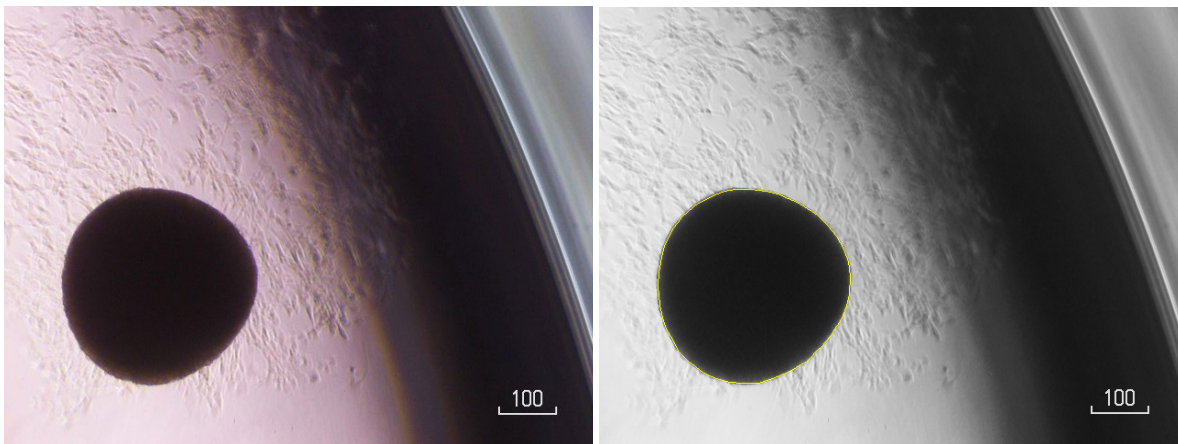
Spheroid volume experiment (E1)
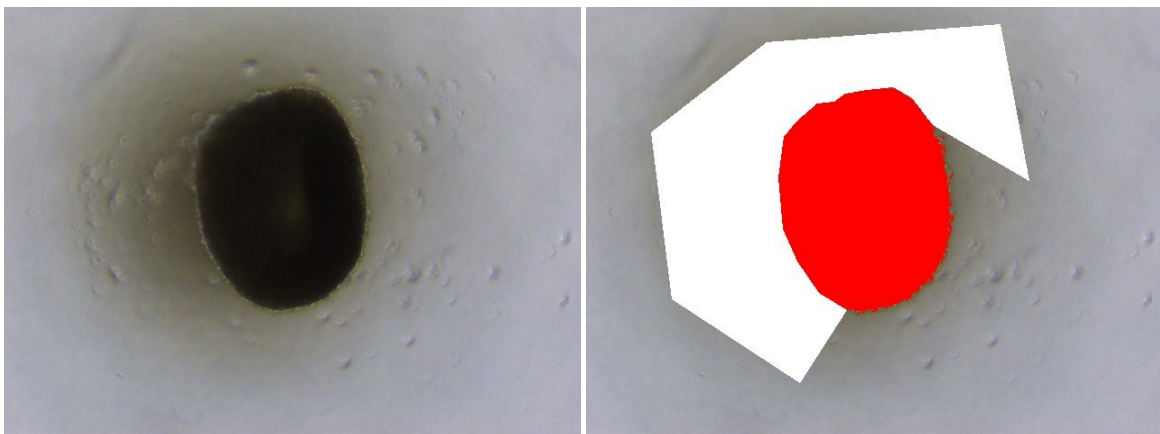
Figure 9: *E1 S3 1.25x105 cells per spheroid. Section (white) was deleted prior to filtration (red).*
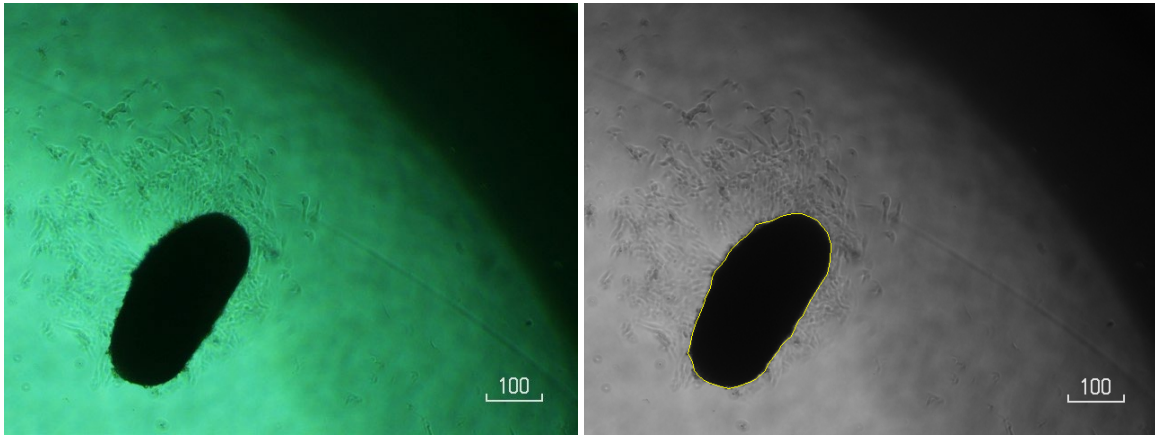
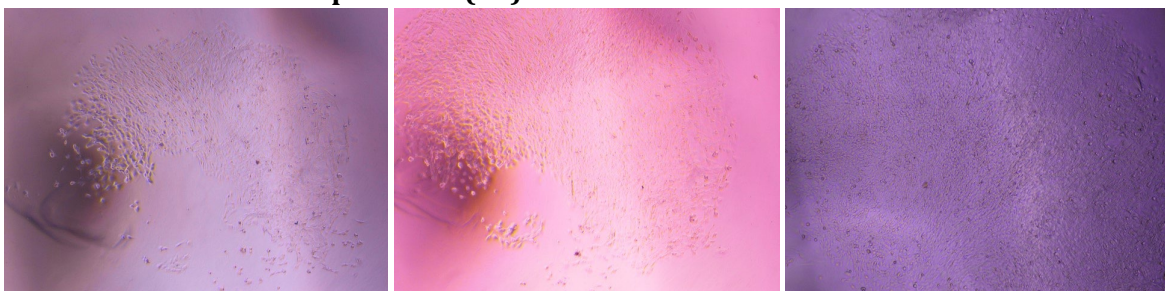*Figure 10:* *E1 S6 1.25x105 cells per spheroid. Analyzed with SpheroidJ.*

*Figure 11:* *E1 S10 1.25x105 cells per spheroid. Left: unfiltered; middle: filtered; right: outlines.*

Figure 12: *E1 S7 2.50x105 cells per spheroid near the edge of the well.*
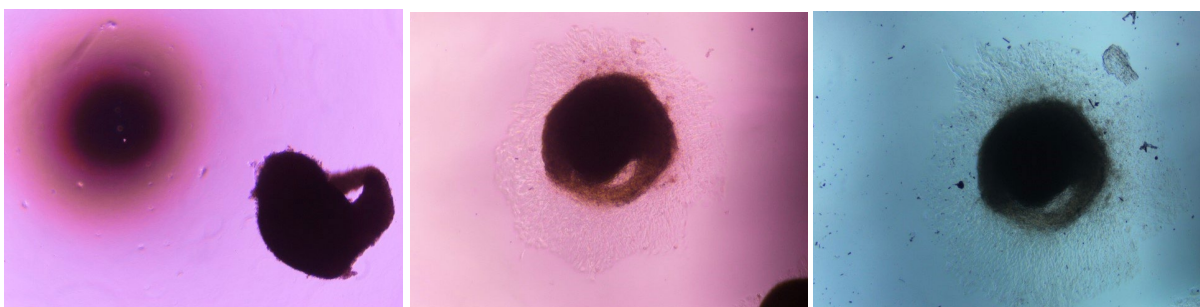
Electrical stimulation experiment (E2)

Figure 13: *E2 S8 (left), S9 (middle), and S10 (right) of the control group. The spheroid was removed from well surface on S7. The remaining cells on well surface proliferated in the following days.*
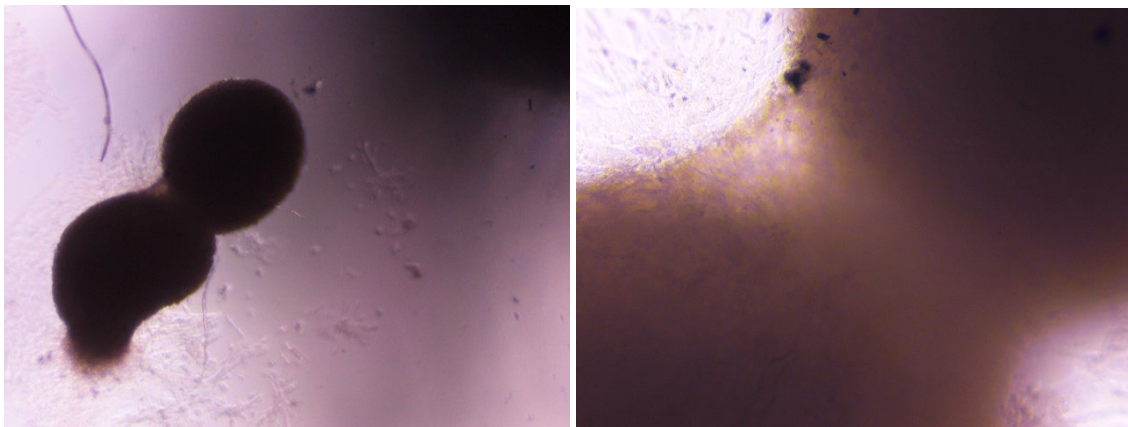
Figure 14: E2 S8 4V. Spheroids merged between S3 and S6. Photo on the left is taken at 4X and right is a 20X magnification.

Figure 15: E2 4V on S3 (left), S6 (middle), and S7 (right). This spheroid was considered an outlier and was therefore excluded from statistical testing on all datasets.
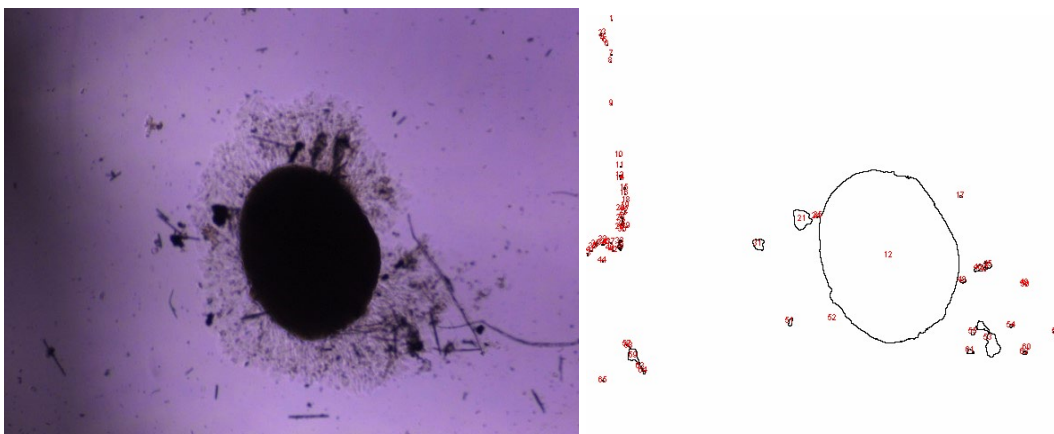
Figure 16: E2 S10 8V. Fibers shown in the original photo are manually removed prior to filtration based on color threshold and particle analysis.